JGR: Biogeosciences

Supporting Information for

High-latitude eddy covariance temporal network design and optimization.

Martijn M.T.A. Pallandt[1†], Martin Jung[2], Kyle Arndt[3], Susan M. Natali[3], Brendan M. Rogers[3], Anna-Maria Virkkala[3], Mathias Göckede[1]

[1]Department of Biogeochemical Signals, Max Planck Institute for Biogeochemistry, Jena, 07745, GER

[2]Department of Biogeochemical Integration, Max Planck Institute for Biogeochemistry, Jena, 07745, GER

[3]Woodwell Climate Research Center, Falmouth, MA 02540, USA

†Current address: Department of Physical Geography, Stockholm University, Stockholm, 114 18, SWE

Contents of this file

Additional Supporting Information (Files uploaded separately)

Captions for Movie S6

Introduction

This supporting information provides several elements to aid the reader or add further details.

- A text and figure that goes into more detail on on of the methods.
- A figure with associated tables to show the locations of ecoregions and extension sites,
- A table that summarized the model runs
- A figure showing the EI mapped for the different temporal model runs.
- A text with a comparison to previous work
- And a movie of the network growth

Text S1.

Realistic pseudo random network distribution

For the depth versus breath analysis we required a new method to assign sitemonths. While the other experiments can be performed with the network in its existing state and limiting additional data points after a certain time, either by tracking months of individual sites (maxX) or by blocking additions after a fixed time (EndX), this experiment requires a reallocation of site activity which makes it susceptible for biases in (random) site selection. For example a selection of few sites with long activity all relatively close in dataspace will have higher overall error than one where these few sites are spread evenly throughout the domain. To mitigate this problem we performed an ensemble run of 20 replicates per time step. A random allocation of sitemonths to site locations and timesteps would result in white noise, while in fact there are distinct patterns in the networks growth and activity (Figure S1.1 B). There is trend of annual growth and seasonality in the network activity (Figure S1.1 C), furthermore when a site is active it is more likely to remain active for consecutive (summer) months. A pseudo random allocation keeps these trends and patterns intact while randomly allocating site's activity within these constrains while allowing us to set the number of active sites.

In the Pseuorandom allocation we filtered out winter months, which for most sites would be gaps and are relatively homogeneous. We then took the linear relation between time and site activity and fitted a sinus function to match the (within summer) seasonality (fig S1.C). For every time step we then know the cumulative total site months, and the site months per time step. Dividing the site months per time step by the total site months results in the relative allocation weights for each time step. These relative allocation weights alone are not enough to reproduce the pattern of site activity, e.g. a site once active will have a more or less continuous activity (during summer months) until it's shut down, with the occasional gap. Therefore once a site month has been allocated to a site, that site's neighboring site months weights are increased by a clumping factor. A clumping factor of zero would result in the neighboring timeslots becoming unavailable as their weight is set to zero. A clumping factor of 1 doesn't change anything whereas an excessively large factor means only the neighboring slots will be selected until all that site's potential allocation slots have been filled. We found a clumping factor of 40 worked best to reproduce the natural patterns, within this order of magnitude the

sensitivity to the clumping factor was low. Once a sitemonth is allotted to a site and timestep its weight is set to zero. And the potential total sitemonths for that timestep is reduced by one. Once a timesteps potential total site months has reached zero all weights in that time slot are set to zero to prevent further allocation. In cases with few sites that require many sites months the total to be allocated site months in the later months can be higher than the number of sites. In this case these potential total site months in access to the number of sites are shifted to the closest (in time) site months that are lower than the number of sites.

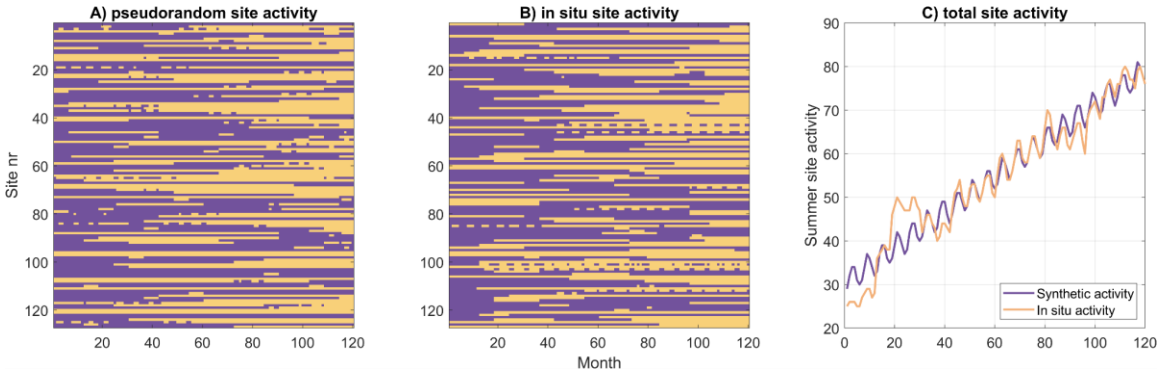

Figure S1.1. A: (left) pseudo random method, B: (center) original data, in both cases purple indicates no data and yellow site activity. C: right) sitemonth activity in-situ in orange, modeled in purple. (Note the different color coding from panels A and B.)

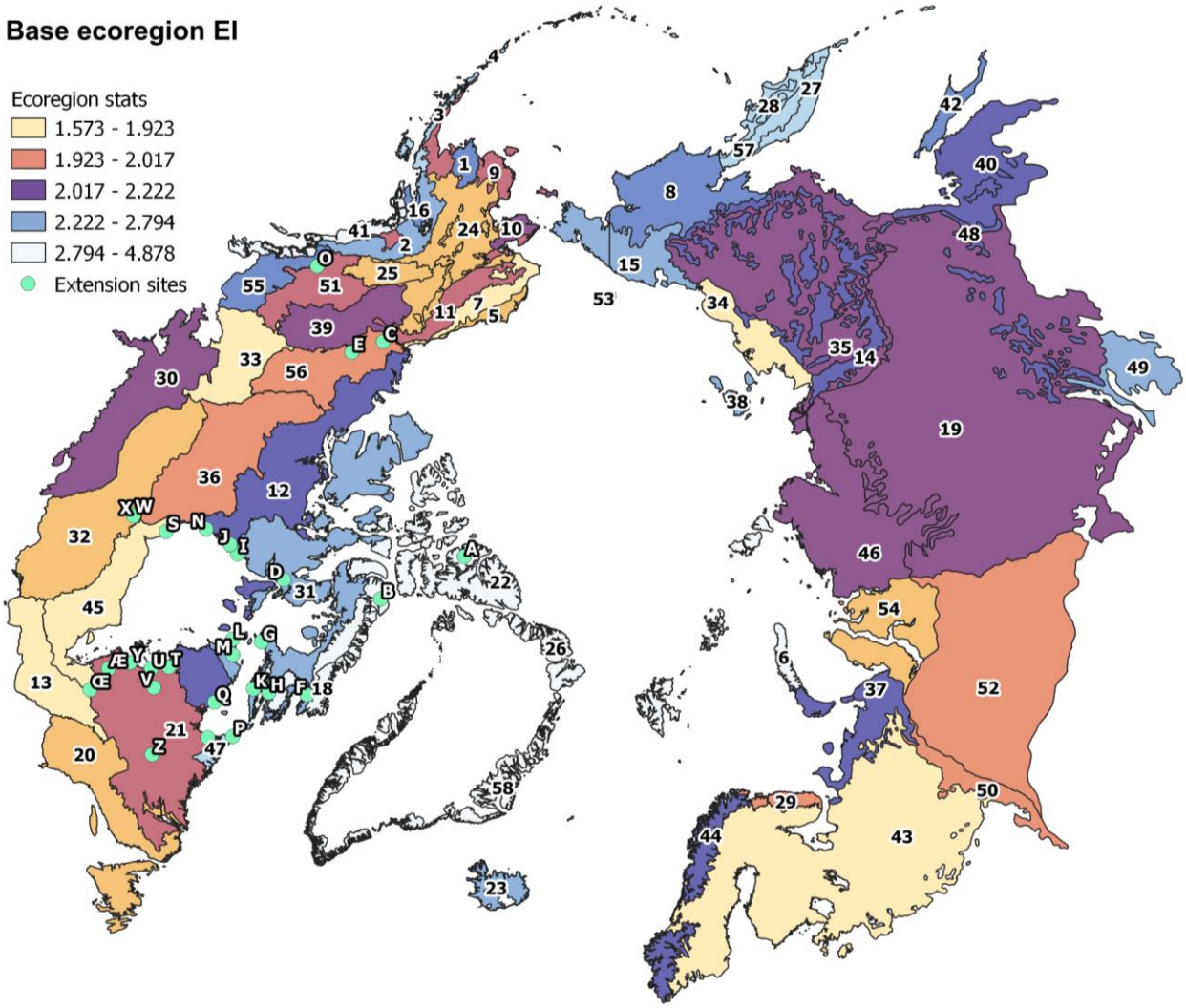

Figure S2. Mean EI per ecoregion, yellow indicates a good representation with low EI values, while purple through white have high EI values. Ecoregions are numbered in black with a white outline, these ID's can be found in table S2.1. Sites are labeled in white letters with a black outline and can be found in table S2.2

Table S2.1. Ecoregion details. ID reflects the number assigned in figure S2, Ecoregion name, Biome and Realm from Dinerstein et al. (2017). EI Statistics of the EI_ref run reflecting the network in 2022.

ID	Ecoregion Name	Biome	Realm	Minimum	Maximum	Range	Mean	Variance	SD
1	Ahklun and Kilbuck Upland Tundra	Tundra	Nearctic	1.11	4.22	3.11	2.27	0.36	0.60
2	Alaska-St. Elias Range tundra	Tundra	Nearctic	0.78	7.46	6.68	2.78	1.15	1.07
3	Alaska Peninsula montane taiga	Boreal Forests/Taiga	Nearctic	1.92	8.05	6.13	3.46	0.71	0.84
4	Aleutian Islands tundra	Tundra	Nearctic	2.28	5.03	2.75	3.36	0.46	0.68
5	Arctic coastal tundra	Tundra	Nearctic	1.08	5.58	4.50	1.77	0.19	0.44
6	Russian Arctic desert	Tundra	Palearctic	2.11	7.84	5.73	4.88	1.11	1.05
7	Arctic foothills tundra	Tundra	Nearctic	0.40	3.16	2.75	1.57	0.15	0.38
8	Russian Bering tundra	Tundra	Palearctic	1.35	4.40	3.05	2.30	0.20	0.44
9	Beringia lowland tundra	Tundra	Nearctic	0.31	3.77	3.46	2.02	0.18	0.43
10	Beringia upland tundra	Tundra	Nearctic	1.34	4.32	2.98	2.05	0.15	0.38
11	Brooks-British Range tundra	Tundra	Nearctic	0.55	3.83	3.28	1.99	0.17	0.41
12	Canadian Low Arctic tundra	Tundra	Nearctic	0.97	5.20	4.23	2.10	0.22	0.47
13	Central Canadian Shield forests	Boreal Forests/Taiga	Nearctic	0.88	3.17	2.29	1.60	0.07	0.27
14	Cherskii-Kolyma mountain tundra	Tundra	Palearctic	1.10	4.61	3.50	2.21	0.24	0.49
15	Chukchi Peninsula tundra	Tundra	Palearctic	1.07	5.18	4.12	2.47	0.55	0.74
16	Cook Inlet taiga	Boreal Forests/Taiga	Nearctic	0.94	4.38	3.44	2.31	0.42	0.65
17	Copper Plateau taiga	Boreal Forests/Taiga	Nearctic	1.51	2.93	1.43	2.01	0.04	0.21
18	Davis Highlands tundra	Tundra	Nearctic	2.05	5.97	3.92	3.88	0.61	0.78
19	East Siberian taiga	Boreal Forests/Taiga	Palearctic	1.04	6.02	4.97	2.04	0.12	0.34
20	Eastern Canadian forests	Boreal Forests/Taiga	Nearctic	0.96	3.33	2.36	1.81	0.06	0.24
21	Eastern Canadian Shield taiga	Boreal Forests/Taiga	Nearctic	1.35	3.78	2.43	1.98	0.06	0.24
22	Canadian High Arctic tundra	Tundra	Nearctic	1.87	6.92	5.05	3.98	1.03	1.01
23	Iceland boreal birch forests and alpine tundra	Boreal Forests/Taiga	Palearctic	1.81	7.55	5.74	2.75	0.54	0.73
24	Interior Alaska-Yukon lowland taiga	Boreal Forests/Taiga	Nearctic	0.84	3.26	2.41	1.80	0.05	0.23
25	Interior Yukon-Alaska alpine tundra	Tundra	Nearctic	0.88	2.90	2.02	1.77	0.04	0.20
26	Kalaallit Nunaat High Arctic tundra	Tundra	Nearctic	2.41	7.14	4.73	4.01	0.57	0.76
27	Kamchatka-Kurile meadows and sparse forests	Boreal Forests/Taiga	Palearctic	1.66	5.37	3.71	3.37	0.58	0.76
28	Kamchatka taiga	Boreal Forests/Taiga	Palearctic	1.78	4.51	2.72	2.88	0.33	0.58
29	Kola Peninsula tundra	Tundra	Palearctic	1.23	3.82	2.58	1.96	0.09	0.30
30	Mid-Canada Boreal Plains forests	Boreal Forests/Taiga	Nearctic	0.47	6.07	5.60	2.06	0.75	0.87
31	Canadian Middle Arctic Tundra	Tundra	Nearctic	1.46	6.38	4.92	2.73	0.39	0.62
32	Midwest Canadian Shield forests	Boreal Forests/Taiga	Nearctic	1.14	8.73	7.59	1.81	0.30	0.55
33	Muskwa-Slave Lake taiga	Boreal Forests/Taiga	Nearctic	0.77	5.11	4.33	1.66	0.07	0.27
34	Northeast Siberian coastal tundra	Tundra	Palearctic	1.11	2.91	1.80	1.74	0.04	0.19
35	Northeast Siberian taiga	Boreal Forests/Taiga	Palearctic	1.13	4.82	3.69	2.02	0.13	0.36
36	Northern Canadian Shield taiga	Boreal Forests/Taiga	Nearctic	1.35	3.08	1.73	1.96	0.06	0.24
37	Northwest Russian-Novaya Zemlya tundra	Tundra	Palearctic	1.53	4.86	3.33	2.16	0.13	0.36
38	Novosibirsk Islands Arctic desert	Tundra	Palearctic	1.81	6.05	4.24	2.73	0.51	0.72
39	Ogilvie-MacKenzie alpine tundra	Tundra	Nearctic	1.32	4.51	3.19	2.05	0.16	0.40

40	Okhotsk-Manchurian taiga	Boreal Forests/Taiga	Palearctic	1.51	3.60	2.09	2.17	0.07	0.26
41	Pacific Coastal Mountain icefields and tundra	Tundra	Nearctic	1.67	9.72	8.05	4.00	1.96	1.40
42	Sakhalin Island taiga	Boreal Forests/Taiga	Palearctic	1.61	3.44	1.83	2.26	0.08	0.28
43	Scandinavian and Russian taiga	Boreal Forests/Taiga	Palearctic	0.45	4.81	4.36	1.76	0.18	0.42
44	Scandinavian Montane Birch forest and grasslands	Tundra	Palearctic	1.21	5.91	4.70	2.18	0.19	0.44
45	Southern Hudson Bay taiga	Boreal Forests/Taiga	Nearctic	0.93	3.04	2.12	1.75	0.06	0.25
46	Taimyr-Central Siberian tundra	Tundra	Palearctic	1.40	4.57	3.18	2.04	0.10	0.31
47	Torngat Mountain tundra	Tundra	Nearctic	1.89	4.16	2.27	2.80	0.16	0.40
48	Trans-Baikal Bald Mountain tundra	Tundra	Palearctic	1.63	3.78	2.15	2.21	0.08	0.29
49	Trans-Baikal conifer forests	Boreal Forests/Taiga	Palearctic	1.58	7.09	5.51	2.65	0.64	0.80
50	Urals montane forest and taiga	Boreal Forests/Taiga	Palearctic	1.24	4.60	3.36	1.96	0.15	0.38
51	Watson Highlands taiga	Boreal Forests/Taiga	Nearctic	1.19	3.18	1.99	1.99	0.05	0.23
52	West Siberian taiga	Boreal Forests/Taiga	Palearctic	1.05	4.04	2.99	1.96	0.15	0.39
53	Wrangel Island Arctic desert	Tundra	Palearctic	1.67	2.61	0.94	1.98	0.02	0.16
54	Yamal-Gydan tundra	Tundra	Palearctic	1.19	3.63	2.44	1.91	0.04	0.20
55	Northern Cordillera forests	Boreal Forests/Taiga	Nearctic	1.47	4.84	3.38	2.27	0.12	0.34
56	Northwest Territories taiga	Boreal Forests/Taiga	Nearctic	1.34	3.29	1.95	1.95	0.05	0.23
57	Kamchatka tundra	Tundra	Palearctic	1.56	5.32	3.76	3.33	0.61	0.78
58	Kalaallit Nunaat Arctic steppe	Tundra	Nearctic	1.61	8.91	7.30	3.95	1.64	1.28

Table S2.2. Expansion site names, check marks indicate the sites selection for the run, fixed means the site had been preselected and would be included before other sites would be selected by the algorithm.

ID	Name	Free	Fixed	Free exclude
A	McGill High Arctic Station	✓	✓	
B	Bylot Island Field Station	✓	✓	✓
C	Tsiigehtchic	✓	✓	
D	Repulse Bay	✓	✓	✓
E	Fort Good Hope	✓	✓	
F	Pangnirtung	✓	✓	✓
G	Kinngait	✓	✓	✓
H	Iqaluit	✓	fixed	✓
I	Chesterfield Inlet	✓	✓	
J	Rankin Inlet	✓	✓	
K	Kimmirut	✓	✓	✓
L	Ivujivik	✓	✓	✓
M	Salluit	✓	✓	✓
N	Arviat	✓	✓	
O	Wolf Creek Research Basin	✓	✓	
P	Port Burwell	✓	✓	✓
Q	Kangirsuk	✓	✓	✓
R	Kangiqsualujjuaq	✓	✓	✓
S	Churchill Fen	✓	fixed	✓
T	Boniface River Field Station	✓	✓	✓
U	Umiujaq	✓	✓	✓
V	Wiyâshâkimî Lake Station	✓	✓	✓
W	Reservoir Site 2	✓	✓	✓
X	Reservoir Site 1	✓	fixed	✓
Y	Whapmagoostui-Kuujjuarapik Research Complex	✓	✓	✓
Z	Schefferville	✓	✓	✓
Æ	Radisson Ecological Research Station	✓	✓	✓
Œ	Lac Le Caron	✓	✓	✓

Table S3. Overview of EI model runs, showing the run name, the full temporal extend and a short description.

EI Run name	Temporal	Description
Baseline	2001 - 2020	In situ network
End10	2001 - 2020	Ending measurements in 2010
End15	2001 - 2020	Ending measurements in 2015
Max12	2001 - 2020	Limiting each site's activity to 12 site months.
Max18	2001 - 2020	Limiting each site's activity to 18 site months.
Max36	2001 - 2020	Limiting each site's activity to 36 site months.
DvB10	2001 - 2010	Site months equal to the network's 2010 state, distributed over 55 to 127 locations in steps of 12.
DvB15	2001 - 2015	Site months equal to the network's 2015 state, distributed over 55 to 127 locations in steps of 12.
DvB20	2001 - 2020	Site months equal to the network's 2020 state, distributed over 55 to 127 locations in steps of 12.
EI ref	2022	In situ network for 2022
Free	2022	Optimized sites selected from 28 sites in Canada
Fixed	2022	3 fixed locations and optimized further from the remaining 26 sites in Canada
Free exclude	2022	Optimized sites selected from 21 sites in Canada
Random	2022	8 site addition, 1000 repetitions where possible
Comparison	2019	In situ network for 2019 based on (Pallandt et al., 2022) site list and domain.

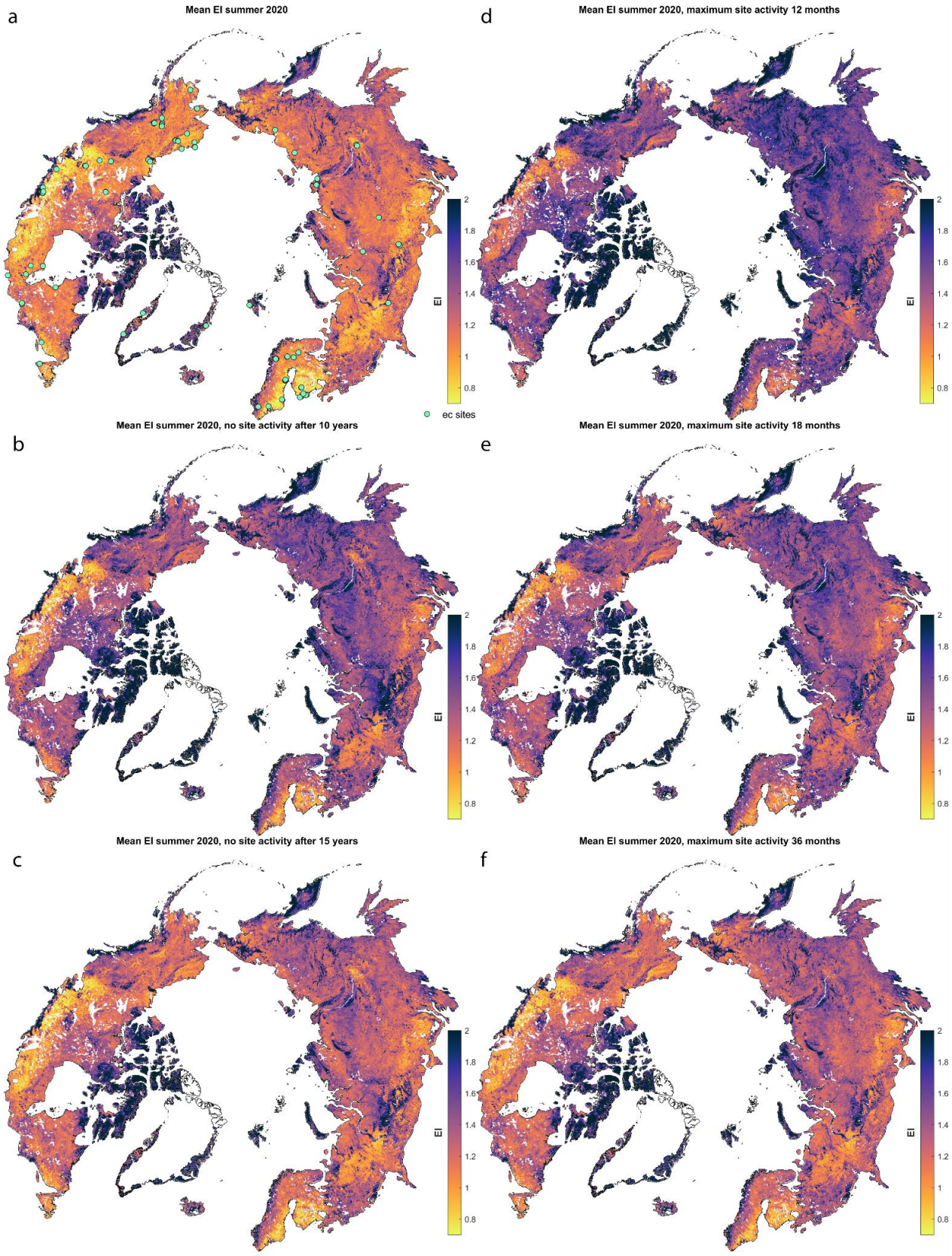
a
Mean EI summer 2020
EI
2
1.8
1.6
1.4
1.2
1
0.8
ec sites
d
Mean EI summer 2020, maximum site activity 12 months
b
Mean EI summer 2020, no site activity after 10 years
e
Mean EI summer 2020, maximum site activity 18 months
c
Mean EI summer 2020, no site activity after 15 years
f
Mean EI summer 2020, maximum site activity 36 months

Figure S4. EI maps for Base Qxx and EndX runs EI based on summer months means of 2020 for the following runs: Base (a), End10 (b), End15 (c), Max12 (d), Max18 (e), Max36 (f). For readability EI values higher than 2 are capped at 2 in this visualization. In the b Base (a) plot tower locations are shown in green circles.

Text S5.

Comparison to previous work

We compare this method with previous work published by (Pallandt et al., 2022) to investigate if these results are robust between different methods. For this purpose, we selected the 'All' subset of the previous study, which contains 120 sites that had been active until 2019, and conducted a separate run for the EI with the same network setup. Since the previous analysis did not consider the temporal aspect, we create a 12 month climatology data by averaging the 20 year monthly explicit variables to a 12 month mean annual cycle, i.e. climatology. For the EI we then take the mean of monthly results calculated over April through September following (Natali et al., 2019) and in line with (Rantanen et al., 2023; Ueyama et al., 2013) for a) summer and b) full year, to create respective maps with no temporal variability. Since the previous analysis allowed for a higher spatial resolution, we downscaled these results to match the 0.0833 degree resolution of this paper and masked out all no-data areas from both maps which most notably included areas south of 60 degrees North and permanent ice sheets.

Between the EI and representativeness metrics we found a correlation of 0.67 for summer and 0.66 for year-round results with a $p>0.001$. This implies that, despite differences in input fields and boundary conditions, results match well overall, and the larger-scale assessments can be confirmed independent of the method applied.

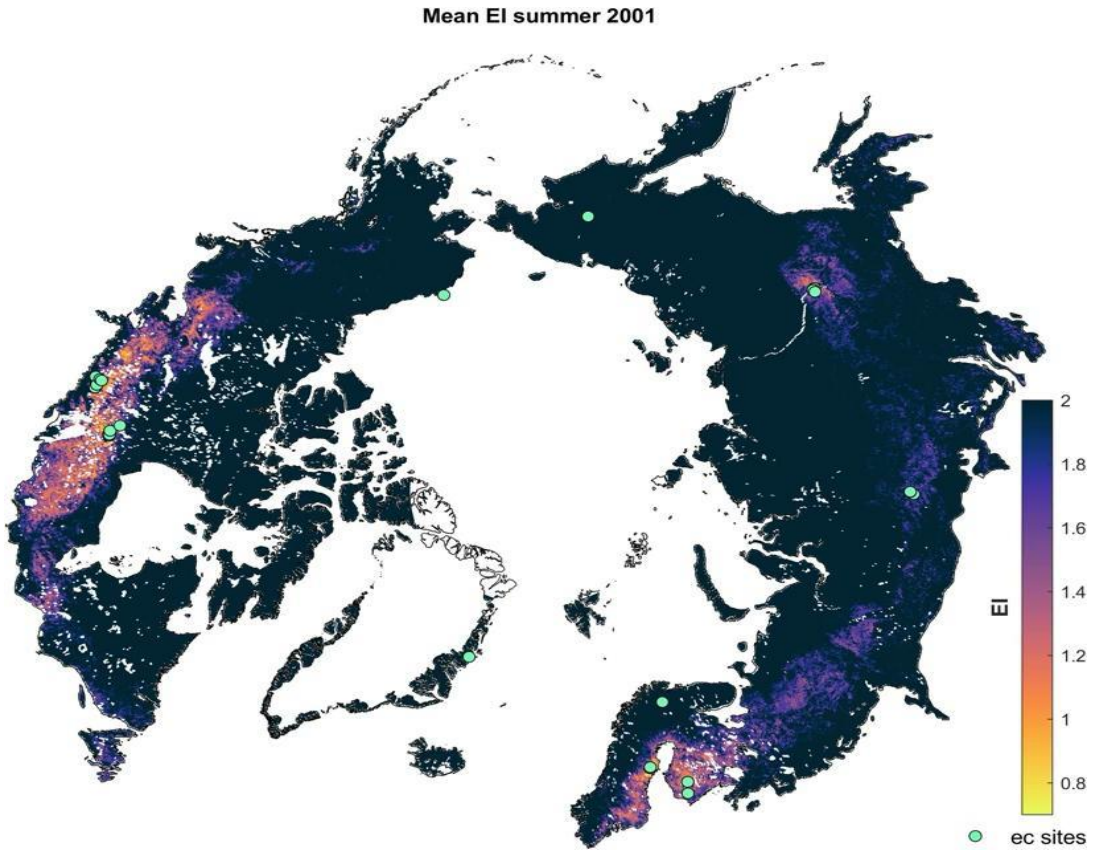

Movie S6. Yearly summer mean EI from 2001 to 2020. Tower locations are shown in green circles. Here the first year is shown.

References

Dinerstein, E., Olson, D., Joshi, A., Vynne, C., Burgess, N. D., Wikramanayake, E., et al. (2017). An Ecoregion-Based Approach to Protecting Half the Terrestrial Realm. *BioScience*, *67*(6), 534–545. https://doi.org/10.1093/biosci/bix014

Natali, S. M., Watts, J. D., Rogers, B. M., Potter, S., Ludwig, S. M., Selbmann, A.-K., et al. (2019). Large loss of CO_2 in winter observed across the northern permafrost region. *Nature Climate Change*, *9*(11), 852–857. https://doi.org/10.1038/s41558-019-0592-8

Pallandt, M. M. T. A., Kumar, J., Mauritz, M., Schuur, E. A. G., Virkkala, A.-M., Celis, G., et al. (2022). Representativeness assessment of the pan-Arctic eddy

covariance site network and optimized future enhancements. *Biogeosciences*, *19*(3), 559–583. https://doi.org/10.5194/bg-19-559-2022

Rantanen, M., Kämäräinen, M., Niittynen, P., Phoenix, G. K., Lenoir, J., Maclean, I., et al. (2023). Bioclimatic atlas of the terrestrial Arctic. *Scientific Data*, *10*(1), 40. https://doi.org/10.1038/s41597-023-01959-w

Ueyama, M., Iwata, H., Harazono, Y., Euskirchen, E. S., Oechel, W. C., & Zona, D. (2013). Growing season and spatial variations of carbon fluxes of Arctic and boreal ecosystems in Alaska (USA). *Ecological Applications*, *23*(8), 1798–1816. https://doi.org/10.1890/11-0875.1